PROCEEDINGS OF SCIENCE

Characteristics of Atmosphere-Skimming air showers relevant for high-altitude radio experiments

Sergio Cabana-Freire,[1,*] **Jaime Álvarez-Muñiz**[1] **and Matias Tueros**[2]

[1]*Instituto Galego de Física de Altas Enerxías (IGFAE), Universidade de Santiago de Compostela, 15782 Santiago de Compostela, Spain*

[2]*Instituto de Física La Plata, CONICET-UNLP, Diagonal 113 entre 63 y 64 , La Plata, Argentina*

E-mail: sergio.cabana.freire@usc.es

Atmosphere-skimming air showers are initiated by cosmic rays with incoming directions located above the Earth's horizon, such that the development of the cascade occurs exclusively in the atmosphere. In this work, we have performed a first characterisation of atmosphere-skimming particle cascades and their associated radio emission using the ZHAireS-RASPASS simulation program. Both the low air density and the orientation of the magnetic field in the region where the shower development takes place are shown to alter the longitudinal and lateral evolution of the particle cascade depending on its geometry. Significant differences in the radio emission appear as a consequence with respect to downward-going air showers, giving rise to unique features whose impact is discussed regarding the exposure of high-altitude detectors and the interpretation of collected data.

10th International Workshop on Acoustic and Radio EeV Neutrino Detection Activities - ARENA2024
11-14 June 2024, Chicago, Illinois, United States

[*]Speaker

PoS(ARENA2024)048

1. Introduction

Atmosphere-skimming (AS) showers are initiated by cosmic rays, and possibly neutrinos or photons, with incoming trajectories such that the shower axis does not intercept the ground and the particle cascade develops entirely through the atmosphere. This type of events have been detected during the four flights of the ANITA experiment [1–4], that recorded several radio pulses with an incoming direction and polarisation consistent with AS air showers emitting radiation through the geomagnetic mechanism. Recent observations of Cherenkov emission aboard the EUSO-SPB2 experiment are also consistent with air showers with AS trajectories [5].

The particular geometries of these showers, that propagate through very rarefied layers of the atmosphere under the effect of the magnetic field, give rise to distinct features in the evolution of the particle cascade and its length scales, as well as in its associated radio emission [6, 7]. In this work, we provide a summary of the main characteristics of AS air showers focusing on their detection using the radio technique aboard balloon-borne experiments. The study was performed through detailed 4D Monte Carlo simulation of the air showers and their radio emission using *ZHAireS - RASPASS* [8], a stand-alone version of the ZHAireS suite capable of simulating air showers with arbitrary incoming directions.

2. Characteristics of Atmosphere-Skimming air showers

An example trajectory of an AS air shower is sketched in figure 1a. Although the geometry is entirely determined by the minimum distance to ground or *impact parameter* b, a different and equivalent description of the geometry will be made in terms of the zenith angle θ of the shower axis passing at an altitude h above the ground. We will focus on the case of balloon-borne detectors, considering only the case of showers passing at altitude $h = 36\,\text{km}$ a.s.l. with different incoming zenith angle θ.

A strong dependence of the density profile along the shower axis with the zenith angle θ arises as a consequence of the almost horizontal geometries of these events. This can be seen in figure 1b, where we show the traversed matter as a function of the distance along shower axis to a detector hovering at $h = 36\,\text{km}$ (placed at $d = 0\,\text{km}$ by definition). The traversed matter (in colour scale) is shown for showers of zenith angle between $\theta = 90°$ to $\theta = 96°$ above which showers intercept ground and are no longer AS. If the shower encounters enough matter to traverse as it propagates towards the detector, it will reach its maximum number of particles at depth X_{max}, typically around $600 - 800\,\text{g/cm}^2$ (blue and green dashed lines in figure 1b). The expected distance between detector and X_{max} changes significantly with the shower zenith angle, a direct consequence of the change in the density profile with θ. For $\theta \lesssim 92°$, showers develop across such rarefied regions of the atmosphere that they do not encounter enough matter to fully develop before reaching the detector. This would open the door to a direct measurement of the particle content of the cascade at early stages of the development, while coherent radio emission is expected to be suppressed. On the other hand, for $\theta \gtrsim 95°$, showers traverse denser regions of the atmosphere reaching their maximum at distances $\gtrsim 1000\,\text{km}$ away from the detector, potentially leaving radio detection as the only viable observation technique, due to the attenuation of the particle cascade and Cherenkov emission in optical wavelengths.

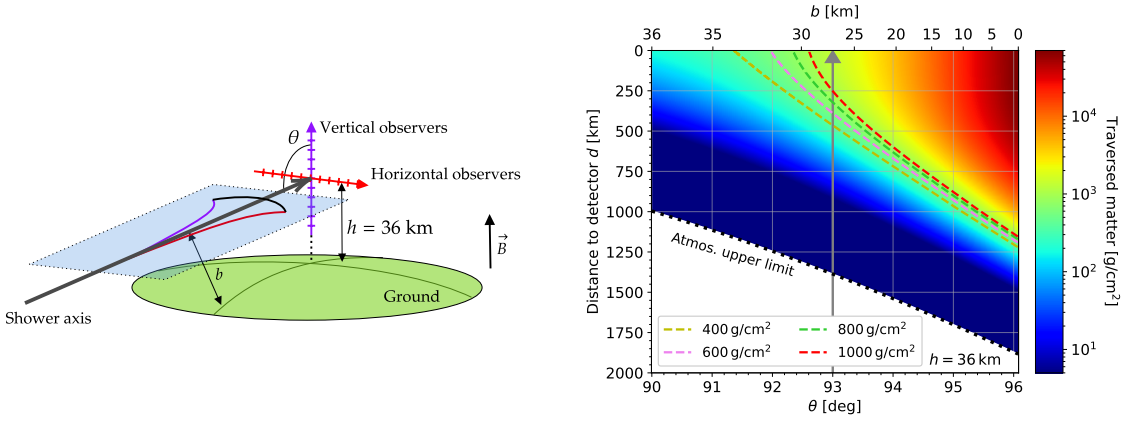

(a) (b)

Figure 1: (a): Example geometry of an AS air shower with zenith angle θ passing at an altitude $h = 36\,\text{km}$. For illustration purposes, the plane where the $\mathbf{v} \times \mathbf{B}$ vector lies, with $\mathbf{v}$ parallel to shower axis, is shown in a light blue colour, for the case of a vertical magnetic field $\mathbf{B}$. In simulations, the radio emission was calculated both along the horizontal (in red) and vertical (in blue) directions. (b): Phase space for development, as a function of the zenith angle θ, for showers passing at an altitude $h = 36\,\text{km}$ (see text for details). The grey arrow illustrates the direction of propagation for the case of $\theta = 93°$.

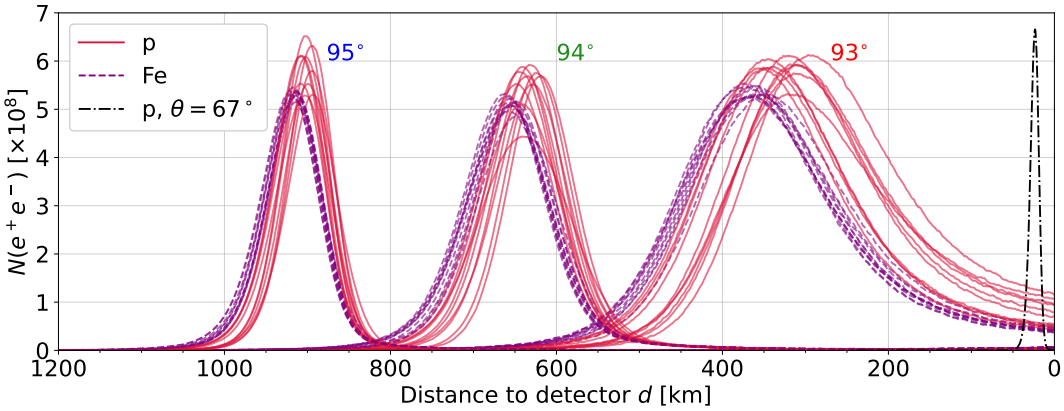

Figure 2: Longitudinal development of the number of $e^{\pm}$, as a function of the distance to the detector (placed at $d = 0\,\text{km}$) for proton (in red) and iron (in blue) showers with primary energy $E_0 = 10^{18}\,\text{eV}$ passing at an altitude $h = 36\,\text{km}$ and different zenith angle. A single downward-going proton shower with $\theta = 67°$ is also shown for comparison (black dashed-dotted line).

In general, the longitudinal development of AS air showers as a function of the traversed grammage is similar to that of downward-going air showers [6]. However, the low densities where the development takes place, typically in the order of tenths of sea level density, give rise to extremely elongated showers that need to traverse increasingly larger distances to complete its development as density decreases with decreasing θ. This can be seen in figure 2, where we show the longitudinal development, as a function of distance to the position of a detector at $h = 36\,\text{km}$, for showers

with different zenith angle and primary particle. The typical longitudinal scale of AS air showers reaches $\sim$ 200 km, an order of magnitude above the typical length scale of downward-going air showers. The longitudinal scale also grows as showers become more horizontal (θ closer to 90°) and propagate higher up in the atmosphere. Naturally, event-to-event fluctuations of a few g/cm^2 in the position of $X_{\max}$ also translate into differences of tens of kilometres.

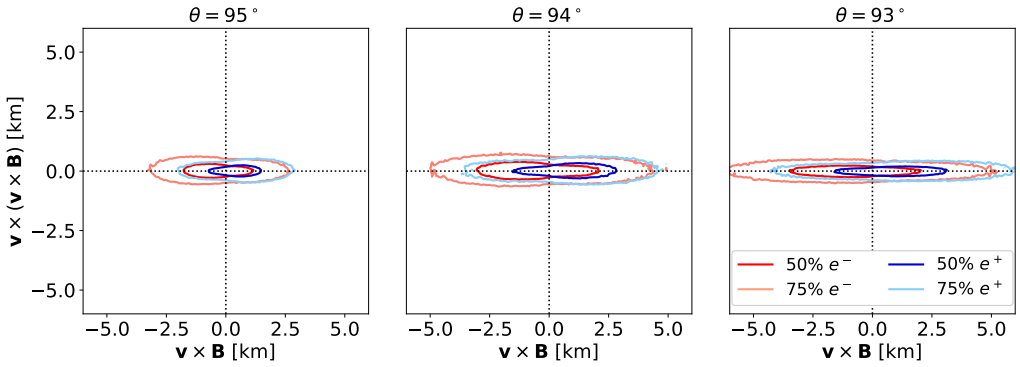

Figure 3: Lateral distribution of e^+ and e^- in a plane perpendicular to the shower axis placed at the position of $X_{\max}$ for three proton showers of primary energy $E_0 = 10^{18}$ eV passing at an altitude $h = 36$ km and zenith angles $\theta = 93°, 94°$ and $95°$. The contour lines represent the regions containing 50% and 75% of e^+ and e^-. The magnetic field in simulations was set perpendicular to the ground plane.

The long distances travelled by the particle cascade under the effect of the magnetic field also have a significant effect on the lateral development of the shower front. As the cascade propagates, the magnetic field tends to spread the shower front along the direction of the Lorentz force. This can be seen in figure 3, where the simulated lateral distribution of $e^\pm$ at shower maximum is shown for three AS air showers of different zenith angle. A clear spread of the shower front along the $\mathbf{v} \times \mathbf{B}$[1] direction is visible. The asymmetry of the shower front grows as the showers become more horizontal (smaller θ). This is due to the larger distances that these showers need to traverse to develop (see figure 2), giving the magnetic field more time to deflect particles, which also do not scatter so often in the rarefied atmosphere.

3. Properties of the radio emission

The distinct geometry and length scales of AS air showers have important consequences on the properties of their associated emission in radio frequencies. Two asymmetries are expected to appear in the lateral distribution (LDF) of the electric field around shower axis. In figure 4 we show the maximum electric field amplitude for the case of a shower with $h = 36$ km and $\theta = 94°$ as a function of distance to the shower axis. The LDFs in two different frequency bands are shown along the horizontal and vertical directions (following the notation of figure 1a), either under the effect of a magnetic field perpendicular or parallel to the ground (left and right panels respectively).

Although the radiation is emitted during the complete shower development, a major part of it adds coherently up to high frequencies when the shower maximum is seen under the Cherenkov

[1] $\mathbf{v}$ being the direction of propagation of the cascade

angle. This gives rise to the two-peak structure of the LDF around axis visible in figure 4, where the maxima corresponds to the positions where individual emissions arrive closer in time. The expected symmetry of the LDF around the shower axis, visible along the horizontal direction, is not present however in the vertical direction, where the LDF appears displaced towards lower altitudes. This effect has its origin in the different optical paths between sources and observers above or below the shower axis, and is also present in very inclined downward-going air showers [9]. Naturally, the travel time of the emitted radiation depends not only on the distance between emitter and observer, but also on the refractive index along the propagation. As a consequence, the positions where the emissions from the whole shower are seen to arrive closer in time depend on the optical path that the radiation has traversed. The net effect is a displacement of the LDF towards lower altitudes. This *refractive* displacement grows as the showers become more inclined (larger θ), since the difference between optical paths above and below axis increases [7]. No frequency dependence is expected in this effect, since the atmosphere is assumed to be non-dispersive in the MHz – GHz frequency range.

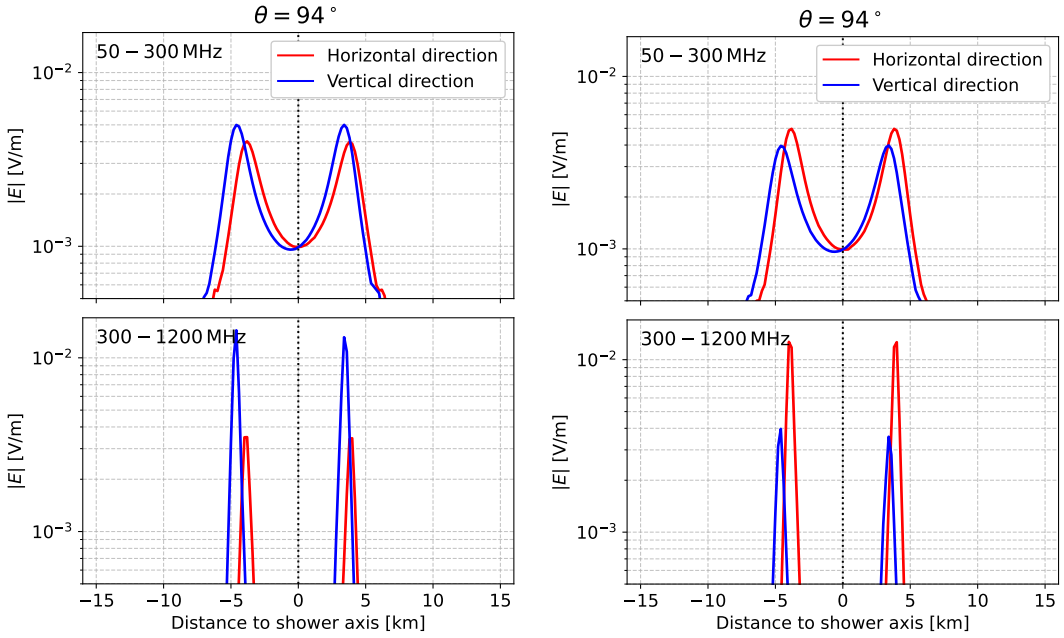

(a) **B** perpendicular to ground

(b) **B** parallel to ground

Figure 4: Lateral distribution of the maximum amplitude of the electric field produced by a 10^{18} eV proton shower passing at an altitude $h = 36$ km with $\theta = 94°$. The LDF is shown both along the horizontal (parallel to ground, in red) and vertical (perpendicular to ground, in blue) directions (see figure 1a). The LDFs are shown in two different frequency bands, namely 50 – 300 MHz (upper panels) and 300 – 1200 MHz (lower panels), for the case of a magnetic field oriented in the perpendicular (a, left panels) or parallel to ground (b, right panels) direction.

A second asymmetry is visible in the maximum values of electric field registered by observers placed either along the horizontal or vertical directions. When the magnetic field is perpendicular to the ground (figure 4a) the maximum electric field is registered along the vertical direction, whereas

the opposite happens when the magnetic field is parallel to ground (figure 4b). The origin of this effect lies in the spread of the shower front in the $\mathbf{v} \times \mathbf{B}$ direction (figure 3). By purely geometric reasons, the time delays between different parts of the shower front are larger if the observer is placed inside the plane where the Lorentz force acts and the shower flattens out, than if the observer was placed outside this plane. In the case of a vertical magnetic field (figure 4a), where the shower front spreads in a plane almost parallel to ground (figure 1a), observers placed along the horizontal direction are more affected by the lateral time delays and receive a signal less coherent than that observed at positions along the vertical direction. The situation is reversed when the magnetic field is horizontal and the shower front flattens out in the vertical direction (figure 4b). Since the frequencies up to which signals can add up coherently are limited by the time delays between different parts of the air shower, this *coherence asymmetry* is a frequency-dependent effect, affecting the shape of the electric field spectra around shower axis [7]. This is visible in figure 4, where the relative difference between the electric field registered along the horizontal or vertical directions is larger when higher frequency components, much more sensitive to any increase in time delays, are considered. The coherence asymmetry also depends on the incoming direction of the air shower, since the flattening of the shower front depends on the density profile traversed by the particle cascade (figure 3) [7].

4. Aperture of balloon-borne radio detectors

The unique properties of the radio emission of AS air showers can have a non-trivial impact at the experimental level. For instance, the asymmetries of the lateral distribution of the electric field around shower axis are translated into asymmetries of the active area for detection around the balloon detector. This is exemplified in figure 5, where we considered proton showers with different energies and impact parameters. The incoming zenith angle of the simulated showers was fixed to the incoming direction of the pulse produced by one of the two *above-horizon* events detected by ANITA IV [4]. The electric field was obtained at the reported height of the payload at the moment of observation of the event. At each point of the detector plane, the colour scale represents the peak electric field in the $200 - 1000\,\mathrm{MHz}$ band, that a shower whose axis passes through that point (i.e. *entering the paper* in figure 5) would produce at the detector, represented by the red marker.

The ring-like structure seen in figure 5 reflects that the emission of the air shower is stronger in a cone around the shower axis, where the individual emissions arrive closer in time and add coherently up to high frequencies. For example, if the shower axis passed exactly through the position of the detector, the received signal would be smaller than if the shower passed slightly to its side, where the detector would see the shower maximum closer to the Cherenkov angle (figure 4). However, the the ring-like shape of the active detection area is not centered at the position the detector, as would be the case if the distribution of the electric field was symmetric around the shower axis. Instead, it appears to be displaced towards higher altitudes with respect to the position of the payload. This effect arises as a consequence of the *refractive* asymmetry discussed in the previous section. When the shower axis is above the detector ($Y > 0\,\mathrm{km}$ in figure 5), the distance between the shower axis and the position that receives the strongest electric field is increased, as a consequence of the displacement of the LDF towards lower altitudes (figure 4). Similarly, the distance between shower axis and the strongest electric field is reduced when the shower passes below the detector.

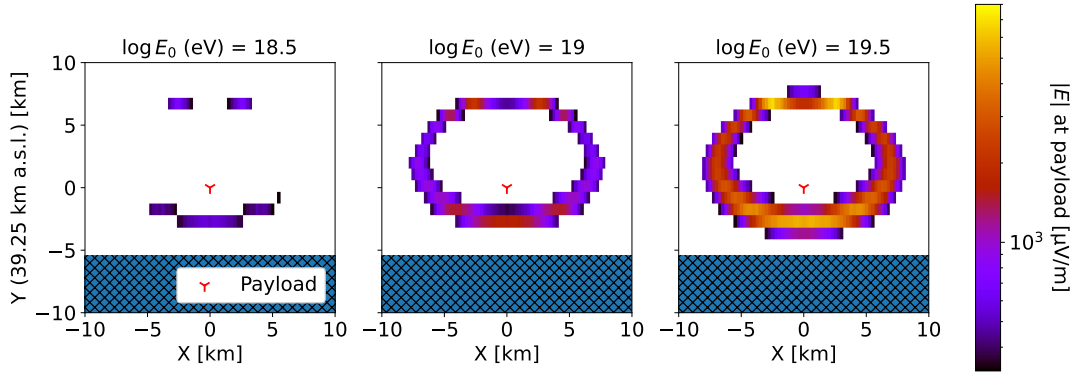

Figure 5: Active detection area around the position of a balloon-borne detector, assuming the payload altitude and shower incoming direction of one of the above-horizon events registered by ANITA IV (ID 973452), for three different primary energies. The colour scale represents, at each point, the electric field that a shower whose axis passes through that point would produce at the position of the payload (red marker). A typical trigger value of 325 μV/m was assumed. The striped blue regions at the bottom of each plot represent incoming geometries with $b < 0$ km that are not visible.

In the considered case, the effect is particularly noticeable given the inclined incoming direction of the event ($\theta = 95.64°$). This asymmetry would favour, in general, the observation of air showers passing above the detector and propagating across lower densities.

A clear difference in the observed electric field appears depending on whether the shower axis passed above or below the detector, or to its sides. This difference has its origin on the *coherence asymmetry*. In the simulated configurations, the considered magnetic field was almost perpendicular to the ground, as in the proximity of the South Pole where the ANITA flights took place. Under the effect of such magnetic field configuration, the shower front would be elongated along the direction parallel to ground (similar to figure 1a, X direction in figure 5). Therefore, if the shower axis passes at an altitude similar to that of the payload, the observer will be placed inside the $\mathbf{v}\times\mathbf{B}$ plane where the Lorentz force acts, the shower front spreads laterally, and the associated time delays are largest. On the other hand, if the detector was placed above or below the shower axis, it would fall outside the plane $\mathbf{v}\times\mathbf{B}$ where the delays seen by the observers are smaller. As a consequence, showers passing to the sides of the detector give rise to fainter signals than those produced by showers leaving the payload above or below their axis. The impact of this effect is particularly noticeable at primary energies such that the emitted signals have amplitudes close to the detection threshold. For instance, in the left panel of figure 5, only those showers passing above or below the detector produce signals above the threshold at the position of the payload. The overall effect would be an increase of the minimum primary energy needed to produce a trigger, depending on the incoming geometry of the air shower, the position of the detector and its frequency range of operation, and the orientation of the local magnetic field.

5. Conclusions

The peculiar geometries of atmosphere-skimming showers give rise to unique characteristics in the evolution of the particle cascade and in the properties of its emission at radio frequencies. The

low atmospheric densities where the development takes place induces extremely elongated showers, propagating across hundreds of kilometres under the effect of the geomagnetic field. The action of the Lorentz force during the propagation of the cascade is also responsible for an elongation of the shower front along the $\mathbf{v} \times \mathbf{B}$ direction.

The almost horizontal geometries of these showers and their length scales have significant effects on their radio emission. The difference in optical paths above and below shower axis give rise to a *refractive* displacement of the LDF towards lower altitudes, while the increased lateral time delays reduce the high frequency content of signals received inside the plane where the Lorentz force spreads the shower front. Both asymmetries in the lateral distribution of electric field around axis can have non-trivial effects at the experimental level, starting with the asymmetries of the active area for detection aboard balloon-borne experiments. Detailed simulations will thus become key to address the impact of these effect on the interpretation of data collected by the next generation of balloon-borne radio detectors, such as PUEO [10] or the POEMMA - Balloon with Radio [11].

6. Acknowledgements

This work has received financial support from Xunta de Galicia, Spain (CIGUS Network of Research Centers, Consolidación 2021 GRC GI-2033 ED431C-2021/22 and 2022 ED431F-2022/15), Feder Funds, Ministerio de Ciencia, Innovación y Universidades/Agencia Estatal de Investigación, Spain (PID2019-105544GB-I00, PID2022-140510NB-I00, PCI2023-145952-2), and European Union ERDF.

References

[1] ANITA Collaboration. Astropart. Phys. 32 (2009) 10. [0812.1920]

[2] ANITA Collaboration. Phys. Rev. Lett. 117 (2016) 071101. [1603.05218]

[3] ANITA Collaboration. Phys. Rev. Lett. 121 (2018) 161102. [1803.05088]

[4] ANITA Collaboration. Phys. Rev. Lett. 126 (2021) 071103. [2008.05690]

[5] JEM-EUSO Collaboration. PoS ICRC2023 (2023) 527. [2310.07063]

[6] Tueros, M. et al. JCAP 07 (2024) 065. [2404.01239]

[7] Tueros, M. et al. PoS ICRC2023 (2023) 349.

[8] Tueros, M. et al. PoS ARENA2022 (2023) 056.

[9] Schlüter, F. et al. Eur. Phys. J. C 80 (2020) 643. [2005.06775]

[10] PUEO Collaboration. JINST 16 (2021) P08035. [2010.02892]

[11] POEMMA, JEM-EUSO Collaboration. PoS ICRC2023 (2023) 1159. [2309.14561]